Development of a Slotless Tubular Linear Interior Permanent Magnet Micromotor for Robotic Applications

Haiwei Lu, Jianguo Zhu, *Senior Member, IEEE*, and Youguang Guo, *Member, IEEE*

Center for Electric Machines and Power Electronics, Faculty of Engineering, University of Technology, Sydney, NSW 2007, Australia

Linear micromotors play a key role in microrobotic systems. They can greatly simplify the drive mechanisms, which is crucial for microsystems. By using permanent magnets, much higher force-to-volume ratio can be obtained than using electromagnets and better drive performance can be achieved. This paper describes the development of a tubular permanent magnet linear motor for the actuation of microrobots. Important design criteria are established by both analytical and numerical methods. The field distribution, the electromagnetic force, and the stator phase winding inductances are analyzed and predicted by the finite-element analysis taking into account the nonlinear properties and saturation effects of the material.

***Index Terms*—Linear motors, linear tubular motors, micromotors, permanent magnet motor, robotics.**

I. Introduction

LINEAR micromotors play a key role in microrobotic systems. Compared to those pneumatic or rotary-motor-based drives, linear motors show significant advantages in terms of efficiency, thrust control, position accuracy, and system volume [1]. Particularly, linear motors can greatly simplify the drive mechanisms, which is crucial for microsystems. By using permanent magnets (PMs) in linear motors, much higher force-to-volume ratio and, hence, better drive performance than using electromagnets can be obtained.

This paper presents the development of a slotless tubular linear interior permanent magnet (TLIPM) micromotor for drive application in microrobots. Important design criteria are established based on the analytical method under several assumptions and the results are compared with the numerical solutions by the finite-element (FE) analysis. The flux density distribution and the electromagnetic force of the motor are analyzed and predicted by the FE analysis. The motor inductances are calculated by considering the nonlinear magnetic properties and saturation effects of the material.

II. Linear Micro Motor Design

A. Motor Structure

Fig. 1 shows the basic configuration of the proposed TLIPM micromotor. The designed external radius R_e of the motor is around 3.5 mm. Three-phase windings are mounted inside the stator core. Due to the small external diameter, the slotless structure is selected for simplicity in construction and better performance. The three-phase windings are arranged as *A-C-B-A-C-B-A-C-B* along the axial direction. The material of the PMs used in the micromotor is Nd–Fe–B, and the material for the stator core is the Glassy Metal, an amorphous soft magnetic ribbon material, which features high magnetic permeability and extremely low core loss. The armature shaft supporting the magnets and pole-pieces is made by nonferromagnetic material (i.e., stainless steel) for some advantages such as reduction of the effective air gap between the stator and the armature, the volume of the PM material, and the moving mass [2].

B. Optimal Design Considerations

In order to determine the suitable thickness of the PMs and the diameter of the moving armature, an analytical analysis is first performed. Although the linear motor has multiple poles, only one pair of poles is needed to be considered when analyzing the performance of the motor. The magnetic circuit per pole pair used for the analysis is shown in Fig. 1.

Under the assumption of infinite magnetic permeability of the iron core and ignoring the leakage flux, by solving the magnetic circuit shown in the figure, the magnetic flux per pole pair ϕ_g can be worked out as

$$\phi_g = \mu_0 \pi H_c \frac{\tau_m}{4g/(2l_m + 2S + g)(\tau - \tau_m) + \tau_m / l_m(l_m + 2S)} \tag{1}$$

where

H_c coercive force of the PM material;
τ pole pitch of the armature;
τ_m width of the PM material;
l_m radial depth of the PM material;
g the gap between the stator and armature;
S radius of the nonferromagnetic shaft.

Therefore, the flux density in the air gap B_g can be estimated by $B_g = \phi_g / A_g$, where A_g is the area of the air gap per pole

$$B_g = 2\mu_0 H_c \frac{\tau_m}{4g + \tau_m(2l_m + 2S + g)(\tau - \tau_m)/l_m(l_m + 2S)}. \tag{2}$$

When keeping the volume of the motor and number of poles unchanged, say, taking l_m, g, and τ as constants, the flux and the

Digital Object Identifier 10.1109/TMAG.2005.855158

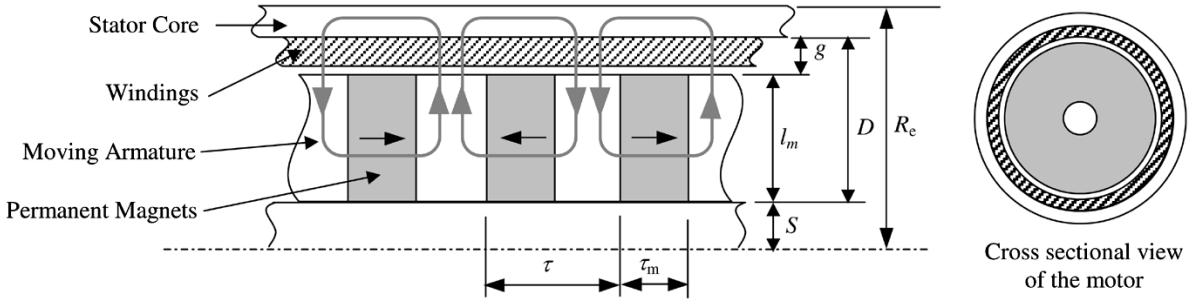

Fig. 1. Configuration of the proposed TLIPM micro motor.

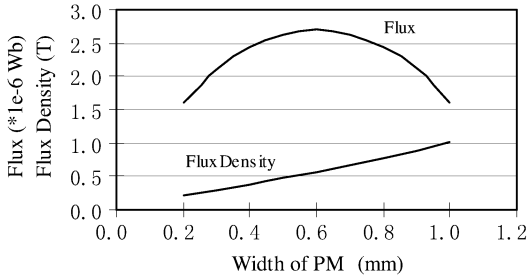

Fig. 2. Flux and flux density in air gap versus width of PM.

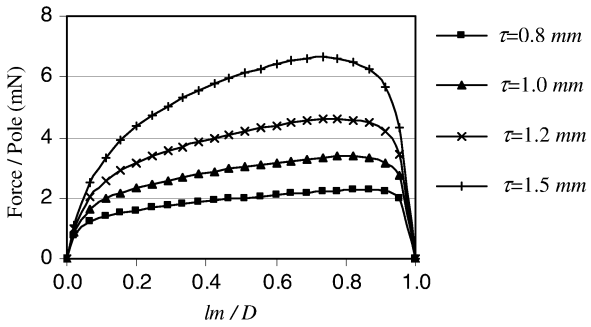

Fig. 3. Electromagnetic force versus the ratio of l_m/D.

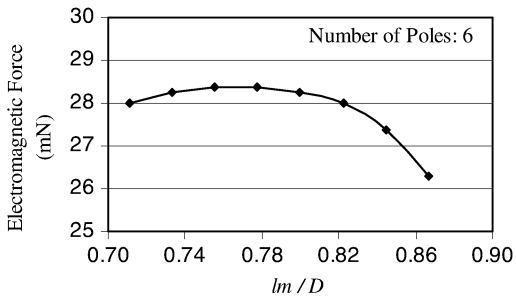

Fig. 4. Electromagnetic force versus the ratio of l_m/D by FE analysis.

flux density in the air gap will vary with the width of the PMs τ_m, as shown in Fig. 2. It is seen that there exists a maximum flux at a certain width of PMs. By applying $d\phi_g/d\tau_m = 0$, it can be found that the magnetic flux per pole pair will be maximum when $\tau_m = \tau/2$.

The electromagnetic force produced in the stator windings can be worked out by $F = \mathrm{BIL}$. Based on the flux density derived in (2) and applying $\tau_m = \tau/2$, the electromagnetic force per pole can be expressed as

$$F_m = \mu_0 \pi H_c J_s k_f \frac{\tau^2 g l_m (l_m + 2S)(2l_m + 2S + g)}{16 g l_m (l_m + 2S) + \tau^2 (2l_m + 2S + g)} \tag{3}$$

where J_s is the current density of the stator windings and k_f the fill factor of the windings. If the radii of the motor and the shaft keep constant, or in other words, the gap D between the stator core and the shaft, as shown in Fig. 1, is constant, by applying $g = D - l_m$, (3) can be rewritten as

$$F_m = \mu_0 \pi H_c J_s k_f \times \frac{\tau^2 l_m (D - l_m)(2S + l_m)(D + 2S + l_m)}{16 l_m (D - l_m)(2S + l_m) + \tau^2 (D + 2S + l_m)} \tag{4}$$

From (4), it is shown that the electromagnetic force is a function of l_m. The variation of the force per pole with l_m is computed and is shown in Fig. 3 by using the ratio of l_m/D. It is noticed that there also exists an optimal value of l_m which makes the force reach its maximum value at the specified pole pitch and motor radius, and it can be found by applying $dF_m/dl_m = 0$ to (4). For the motor presented in this paper, the optimal ratio of l_m/D is found to be 0.778 and the maximum force per pole is 4.6 mN when the current density of the windings J_s is set to be 6 A/mm ^{2}.

The numerical method is applied to compare with the analytical solution. By a two-dimensional (2–D) FE analysis, the flux density in the air gap and the electromagnetic forces produced in the stator windings are calculated. When applying $\tau_m = \tau/2$, the effective flux density in the air gap is found to be 0.47 T, which is close to the analytical result. The electromagnetic force is calculated at different l_m/D ratios as shown in Fig. 4 and the maximum force occurs near $l_m/D = 0.78$. It is seen that the numerical results agree well with the analytical results.

III. Motor Flux Density and Force

Since the moving armature of the micromotor is deliberately designed shorter than the stator so that it can move back and forth within the stator, the distribution of the resultant flux density in the air gap varies with the position of the armature. Consequently, the produced electromagnetic force is also a function of the position of the armature. A 2-D FE model is established to analyze the flux density in the air gap at different armature positions. Fig. 5 shows the flux distribution when the armature is in the middle of the motor. The nonlinear properties of magnetic core are considered in the analysis.

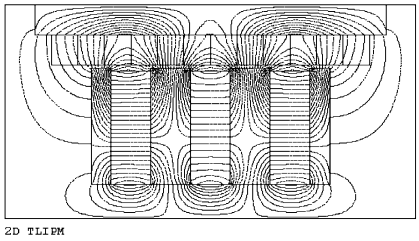

Fig. 5. 2-D flux distribution in the TLIPM.

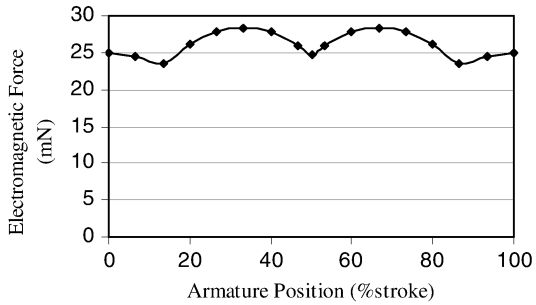

Fig. 6. Motor force versus armature positions.

Based on the analysis of the flux density distribution in the air gap at different armature positions, the produced electromagnetic force can be predicted. The results can provide an optimal current commutation scheme for the motor controller. Fig. 6 shows the motor forces at different armature positions when applying a current density of 6 A/mm^2 and a suitable current switching sequence as $A\bar{B} \rightarrow \bar{B}C \rightarrow \bar{A}C \rightarrow \bar{A}B$. The three positions which generate the lowest forces will be used as the current commutation points.

IV. Stator Winding Inductances

The stator winding inductance is one of the most important parameters for the motor modeling, performance simulation, and controller design. In this paper, the energy method is applied for the inductance computation. However, due to the nonlinear properties of the magnetic core, it is difficult to use 2-D FE model to work out the stored magnetic energy in such a tubular structure. Thus, a three-dimensional (3-D) FE model is applied and during the analysis, both the nonlinear and saturation effects are considered to improve the accuracy of calculation.

Because of the nonlinear properties of the Glassy Metal, it is necessary to find out the operation point set by the PMs before the magnetic energy produced by the stator current can be correctly obtained. Fig. 7 shows the flux density produced only by the PMs via a 3-D nonlinear FE model. Based on the results, the magnetic flux density in each part of the magnetic core of the motor can be obtained and the related magnetic permeability can be found. Table I lists the relative permeability in different magnetic core regions.

From Table I, it is shown that the armature core is saturated, especially the pole-pieces in the middle of the armature. Taking the results as the operation point, the magnetic energy generated by the stator winding current is calculated by ignoring the PMs, and the inductances of the windings can then be worked out by the energy method. The computational results at different armature positions are shown in Table II. It is seen that inductances will not change much at different armature positions.

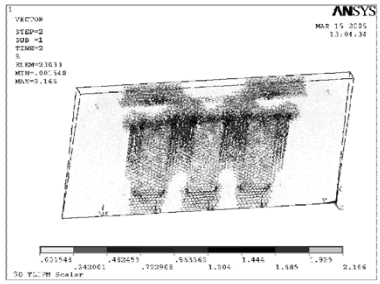

Fig. 7. 3-D FE model of TLIPM with flux density distribution.

TABLE I
Relative Permeability in Different Motor Parts

Armature core Upper	Armature core 2nd layer	Armature core 3rd layer	Armature core Bottom	Stator core
258	121	121	275	478400

TABLE II
Stator Winding Self and Mutual Inductances (Unit: μH).

Position	L_a	L_b	L_c	L_{ab}	L_{bc}	L_{ac}
0% stroke	15.0	15.0	14.8	2.43	7.59	7.62
50% stroke	14.8	14.8	15.2	3.06	7.37	7.37
100% stroke	15.0	15.0	14.9	2.43	7.62	7.58

It is noted that the mutual inductance between phases A and B L_{ab} is much smaller than the other two mutual inductances. This is due to the unsymmetrical distribution of the phase windings, which makes the coupling effect between phase A and B less than that of others.

V. Conclusion

A PM linear motor has been developed for linear motion microrobotic systems. Important design criteria are established by the analytical study of the flux and electromagnetic force of the motor. Numerical solutions are applied to compare with the analytical analysis and the results show a good consistency. The forces of the micromotor are predicted at different armature positions based on the FEA and an optimal commutation scheme is obtained for the motor controller. The results show that the proposed micromotor has a satisfactory force capability. In addition, the inductances of the motor are calculated by considering the nonlinear properties and saturation effects of the material, which will be very helpful to the design of the motor controller.

References

[1] N. Bianchi, S. Bolognani, and F. Tonel, "Design consideration for a tubular linear PM servo motor," *EPE J.*, vol. 11, no. 3, pp. 41–47, Aug. 2001.

[2] J. Wang, D. Howe, and G. W. Jewell, "Analysis and design optimization of an improved axially magnetized tubular permanent-magnet machine," *IEEE Trans. Energy Convers.*, vol. 19, no. 2, pp. 289–295, Jun. 2004.

[3] B. Lequesne, "Permanent magnet linear motors for short strokes," *IEEE Trans. Ind. Applicat.*, vol. 32, no. 1, pp. 161–168, Jan./Feb. 1996.

Manuscript received February 7, 2005; revised March 18, 2005.